High-speed photographic analysis of the soil disturbance affected by subsoiler rake angle

Chengguang Hang[1], Yuxiang Yao[1], Yuxiang Huang[1,2*], Wei Li[1], Ruixiang Zhu[1,2]

(1. *College of Mechanical and Electric Engineering, Northwest A&F University, Yangling, China, 712100*;
2. *Shaanxi Engineering Research center for Agricultural Equipment, Yangling, China, 712100*)

Abstract: Rake angle is a key parameter of subsoiler structural design and has important impacts on subsoiler performance. In this study, the high-speed photographic technique was used to understand the mechanisms by which the rake angle of an arrow subsoiler (angles of 18°, 23°, and 28°) impacted soil disturbance. The following results were obtained. (1) Rake angle was the main factor that influenced the soil disturbance process. Changing the rake angle could induce changes in the interactions between the subsoiler and soil, impacting soil disturbance performance. (2) Rake angle had significant impacts on the soil disturbance state. The horizontal soil disturbance distance increased and the vertical soil elevation decreased when the rake angle was increased. For a fixed soil loosening strip length, the soil disturbance resulting from a subsoiler rake angle of 23° was 1.14 and 1.03 times greater than the soil disturbance that resulted from rake angles of 18° and 28°, respectively. (3) The rake angle also had significant impacts on the soil disturbance results. When the rake angle was 28°, the subsoiler soil disturbance rates in the top 10 cm soil layer and the entire top soil layer were 92.89% and 99.13%, respectively, which were greater than when the rake angles were 18° and 23°. The rake angle of a subsoiler influenced the soil disturbance. An appropriate rake angle is critical to ensure a high-quality cultivation. This paper provides the information for making decisions regarding subsoiler design and structural parameter optimization.

Keywords: subsoiler, rake angle, soil loosening, high-speed photography, experiment

Citation: Hang, C., Y. Yao, Y. Huang, W. Li, and R. Zhu. 2017. High-speed photographic analysis of the soil disturbance affected by subsoiler rake angle. Agricultural Engineering International: CIGR Journal, 19(2): 42–50.

1 Introduction

Long-term shallow rotary tillage and ploughing severely degrade farmland soil structure and result in the formation of a plough pan with a dense texture under the tillage layer, which impedes crop root development and water and nutrient uptake and the sustainable development of agriculture (He et al., 2009; Zheng et al., 2015). Mechanical subsoiling can effectively improve the structure of the soil, break up the plough pan, improve the ability of the soil to conserve water, and promote crop growth (Naeem et al., 2007; Li et al., 2014; Li et al., 2015; Wang et al., 2015). In 2010, the Central Government Document No. 1 requested that the government should "greatly promote mechanical subsoiling", which resulted in subsoiling subsidy policies. In accordance with the requirements of modern quality and efficient agricultural development, subsoiling should be performed every three years. However, poor operation quality and soil disturbance widely occur due to the poor quality of currently available subsoiling equipment. Thus, studying soil subsoiling disturbance mechanisms can effectively resolve this issue.

Rake angle is an important parameter in subsoiler structural design and has important impacts on subsoiler operation quality (Godwin, 2007; Xue et al., 1987). Researchers have conducted many studies on rake angle effects. For example, Godwin and O'Dogherty (2007) used rake angle, subsoiler distance, and tillage depth parameters to establish a subsoiling tillage resistance prediction model. Badegaonkar et al. (2010) studied the

Received date: 2016-03-16 **Accepted date:** 2017-05-04

*** Corresponding author: Huang Yuxiang,** PhD, Associate Professor, Research focuses on agricultural Engineering, Northwest A & F University, Yangling, Shanxi 712100, China. Tel: 029-87091111. Email: hyx@nwsuaf.edu.cn.

impacts of subsoiler angle and length on tillage quality under simulation conditions. Mouazen and Nemenyi (1999) used subsoiler rake angles of 15°, 23°, and 31° during subsoiling to ensure the effectiveness of simulation results. Shahgoli et al. (2009, 2010) studied the impacts of oscillation amplitude, angle, and traction speed changes in tillage resistance, indicating that a rake angle of 22.5° and a traction speed of 3 km h^{-1} resulted in an optimal resistance reduction effect. In addition, Awad-Allah et al. (2009) studied the proportional relationships between tillage speed, soil-entry angle and tillage resistance using a tillage depth of 30 cm. Xue et al. (1987) indicated that soil disturbance performance of subsoiler was poor when the soil raising (soil-entry) angle was too small and suggested that subsoiler rake angles of 18°-23° were optimal. When studying the segmented soil active force vibration drag reduction mechanism, Xin et al. (2014) discovered that parameters such as rake angle influenced the subsoiling operation resistance by changing the soil force. Zhang et al. (2014) designed a bionic anti-drag subsoiler by imitating muss claws (using a rake angle of 24°) and studied the relationships between structural parameters of subsoiler handles and blades, the curvature of the soil-cutting edge of a subsoiler handle, depth ratio, soil-entry angle, and soil physical properties, including resistance to tillage. Qi et al. (2015) used arrow, wing, and chisel shaped subsoilers to study the impacts of subsoiler tine shape on subsoiling tillage resistance using a rake angle of 28°. The rake angle specified in JB/T 9788-1999 "Chiselling Subsoiler and Handle of Chiselling Subsoiler" for accurate subsoiling is 23° (JB/T 9788-1999). When considering currently available studies and practical applications, the range of rake angles required to ensure optimum subsoiler performance is usually within 18°~28°. The above studies mainly focused on the influences of rake angle on tillage resistance and operation performance. Few studies have been reported regarding the mechanisms by which rake angle impacts soil disturbance.

Therefore, a high-speed photographic technique was used to understand the mechanisms by which the rake angle of an arrow subsoiler (angles of 18°, 23°, and 28°) impacted soil disturbance. It aimed to provide information for making decisions regarding subsoiler design and structural parameter optimization.

2 Mechanisms of rake angle impacting soil disturbance

2.1 Influences of rake angle on subsoiler and soil interactions

The shearing, stretching, and compressing effects experienced by soils under the external pressure of a subsoiler are mainly responsible for soil failure and crushing (Perfect et al., 2002; Ibarra et al., 2005). The compression and cutting imposed by the subsoiler when a tractor pulls the subsoiler are mainly responsible for soil disturbance. As an important subsoiler structural parameter, the rake angle significantly influences the interactions between the subsoiler and soil.

During subsoiling, the subsoiler tine mainly experiences a compression force, F, on its surface (perpendicular to the bevelled tine of the subsoiler) and the frictional force, f, between the soil and subsoiler surface (along the bevelled surface of the subsoiler tine and towards the back of the subsoiler). Here, F is the force that crushes and uplifts the soil, and f is the force that induces the soil to flow toward the back of the subsoiler along its surface. The directions of both forces are influenced by changes in the rake angle, α. The relationship between the subsoiler tine force and the rake angle is shown in Figure 1.

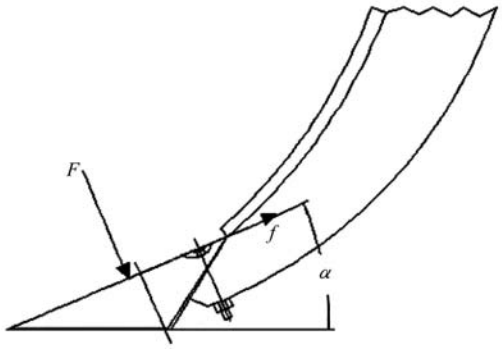

Figure 1 Force analysis of tine in the subsoiler

According to Newton's third law and McKyes (1985), the soil experiences compression force, F', and frictional force, f', from the subsoiler tine surface. Force F' can be decomposed into soil pushing force, F'_x in the horizontal direction and soil uplift force, F'_y, in the vertical direction, as shown in Figure 2.

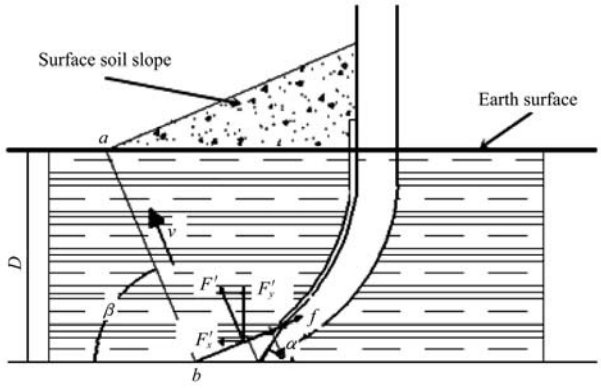

Figure 2 Analysis of interaction between subsoiler and soil

The relationships between F'_x, F'_y and α are

$$F'_x = F' \cdot \sin\alpha \quad (1)$$

$$F'_y = F' \cdot \cos\alpha \quad (2)$$

As shown by Equations (1) and (2), F'_x increases and F'_y decreases as α increases. Thus, the pushing force of the subsoiler on the soil increases when the rake angle increases and the soil uplift force decreases as the soil-entry angle increases.

In addition, during the subsoiling process, the crushed soil flows in the direction of f', and as the rake angle increases, the angle between the subsoiler frictional force on the soil in the direction of f' and the horizontal plane will increase. This change will alter the soil flow process and induce changes in the intra-soil disturbance.

As shown above, changes in rake angle will induce changes in the interactions between the subsoiler and soil system, which will influence the soil disturbance performance of the subsoiler.

2.2 Influence of rake angle on soil disturbance

Due to the interactions between the subsoiler and soil in the subsoiling process, the soil will move forward and upward perpendicular to the tine surface of the subsoiler and will form a soil failure surface, *ab*, passing the tip of the subsoiler tine towards the direction of soil movement (Figure 2). The direction of soil movement is influenced by the direction of the soil uplift force, F'. The angle between the soil uplift force, F', and the horizontal plane is 90°-α. Thus, the angle between the soil movement and horizontal plane decreases as the rake angle increases, which increases the range of the failure surface, *ab*. However, when the rake angle is small, the soil uplift by the subsoiler is greater than the pushing effect. In this case, the height of the raised soil is large and the horizontal range is small. Moreover, when the rake angle is large, the subsoiler pushing effect is greater than the uplift effect, which results in a larger horizontal soil disturbance range and lower soil uplift. From the above discussion, the influences of rake angle on soil movement direction and the subsoiler pushing and uplift effects are mainly responsible for changes in the horizontal and vertical soil disturbance.

The amount of soil disturbance reflects the amount of soil structural failure in the subsoiling process and defines the cross-sectional area of disturbance, *S*, and the subsoiling strip length, *L*. Among these parameters, *S* is influenced by the average width of soil disturbance, *B*, and the disturbed soil thickness, *d*. Without considering the intra-soil disturbance, *B* is influenced by the wing opening angle of the subsoiler tine. The disturbed soil thickness, *d*, is mainly influenced by subsoiling depth (*D*), α, and the soil grain front tilting angle (β), as shown in the following relationship (Wang, 2011):

$$d = D\frac{\sin(\alpha+\beta)}{\sin\beta} \quad (3)$$

As shown in Equation (3), when the subsoiling depth is fixed, *d* is influenced by α and β. Studies have shown that β is mainly influenced by soil type, and its relationship with the internal soil frictional angle, φ, is (Gill and Vanden Berg, 1967):

$$\beta = \frac{1}{2}(90° - \varphi) \quad (4)$$

Thus, for a specific soil, β can be considered a constant, and *d* is influenced by α; thus, the subsoiler soil disturbance is mainly influenced by α.

Meanwhile, the movement of the subsoiler at different rake angles in the soil is similar to front cleats with different wedge angles cutting into the soil under a pulling force. When the rake angle is too large or small, the soil cone and soil heel form where the subsoiler tine and handle are connected, which changes the interaction of the subsoiler with the soil and alters the amount of soil disturbance. Farther from the subsoiler, changes in rake angle will induce changes in the outlined sectional area of soil disturbance due to the effects of the cosine of the rake angle and the internal soil frictional force on the disturbed soil outline width, which in turn changes the

amount of soil disturbance.

3 Materials and methods

3.1 Experimental materials

The test soil was classified as Lou soil (heavy loam), which was an agriculture soil developed from loess soil parent material (Yang et al., 2012). The dry bulk density and water content of the topsoil were 1.346 g cm^{-3} and 11.9%, respectively (Huang et al., 2015).

Currently, subsoiling is used for the long-term cultivation of land. Using arrow-shaped subsoilers for cultivation can effectively reduce subsoiling resistance and improve soil disturbance performance. Thus, an arrow subsoiler tine was chosen in this study. The subsoiler tine had a side wing opening angle of 115°, a circular arc subsoiler shank with a cutting edge angle of 60° and a thickness of 30 mm. Arrow subsoiler tine and circular arc subsoiler are shown in Figure 3.

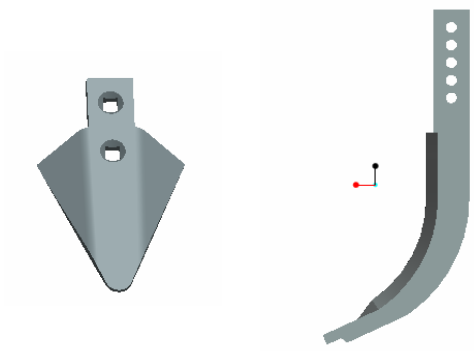

Figure 3 Arrow subsoiler tine (left) and circular arc subsoiler shank (right)

The experiment was conducted using a digital soil bin test bed in the College of Mechanical and Electric Engineering at Northwest A&F University. The test bed was composed of a soil box, electrical powered four-wheel drive trolley, tracks, instrumentations, a stepless speed control system, a kinetic parametric remote sensing system, and various types of sensors and hydraulic systems. The dimensions of the soil bin were 26 m × 2.1 m (track gauge) × 0.7 m (length × width × height). To ensure consistency of the test process, the first 3 m was used as an acceleration region and the last 3 m was used as a deceleration region. Thus, the middle 20 m was used as the effective test distance.

During the soil bin test, the soil in the bin was prepared using the layered processing method according to field soil environmental parameters to ensure that the soil conditions in the bin were consistent with the soil conditions in the field. First, 20 cm of soil was removed from the bin, a 1GQN-125 rotary tiller was used to till the remaining soil, and a vibration compactor was used to compress the remaining soil to a density of 10-20 kg cm^{-2}. Second, water was sprayed evenly on the compressed soil and part of the removed soil (approximately 10 cm) was placed back into the bin. The topsoil layer was tilled using a rotary tiller after three days of water permeation. Finally, the remaining soil was placed in the bin and a compression roller was used to achieve a density of 5-10 kg cm^{-3} in the top soil layer (0-20 cm). The soil water content was maintained at approximately 12% during the soil preparation process. The compression roller and water content measurement processes are shown in Figure 4.

Figure 4 Soil preparation unit (left) and soil parameters measurement device (right) in soil bin

3.2 Research methods

3.2.1 Soil disturbance evaluation index

Soil-disturbance rate is an important index for evaluating the performance of a subsoiler, and it reflects the degree of soil disturbance in the subsoiling strip. This study used the soil-disturbance rate in the 10 cm depth and full tillage layer (30 cm) after subsoiling as an evaluation index to determine the influences of subsoiler rake angle on soil disturbance performance. The method used to measure the soil-disturbance rate is described below.

After subsoiling, a point was marked in each track and soil samples were collected from the subsoiling strip along the direction of subsoiling. In the area of 0.5 m × 0.5 m, the weight of the total clod, all maximum edge of the cold which are less than 4cm within 10cm of the soil and the maximum edge of the cold which is less than 8cm in the whole cultivation layer was determined

respectively. The rate of broken soil was calculated using Equations (5) and (6) (JB/T 10295-2014).

a) Top tillage layer (0-10 cm):

$$C_{10} = \frac{G_{s10}}{G_{10}} \times 100\% \quad (5)$$

where, C_{10} is the soil-disturbance rate, %; G_{s10} is the total mass of area with the longest side length less than 4 cm, kg; and G_{10} is the total soil mass, kg, in the tillage layer within 10 cm of the surface.

b) Full tillage layer:

$$C = \frac{G_s}{G} \times 100\% \quad (6)$$

where, C is the soil-disturbance rate, %; G_s is the total mass of the area with the longest side length less than 8 cm, kg; and G is the total soil mass, kg, in the full tillage layer.

3.2.2 High-speed photography technique

The high-speed photography technique has been widely used in the agricultural sector (Quan et al., 2013; Ouyang et al., 2014). During the subsoiling process, it is difficult to accurately observe the movement and trajectory of soil with the naked eye; thus, an I-SPEED TR high-speed camera was used to record the subsoiling process under different rake angles using a resolution of 2000 pictures/s. The recorded process was played back using the *I-SPEED Suite* software. Through image analysis of the overall images and a specific time image, the influences of the subsoiler rake angle on soil disturbance state and soil disturbance range were studied.

The test was conducted using rake angles of 18°, 23°, or 28°, a tillage depth of 300 mm, and a tillage speed of 3 km h^{-1}. A high-speed camera was used to record the subsoiling process to determine the influences of rake angle on soil disturbance. The soil-disturbance rate was measured using the methods described in the section 2.2.1. The profiling method was used to map cross sections from the surface to the subsoiling furrow. The resulting map was used to calculate the soil disturbance areas. The high-speed photographic recording process and the post-subsoiling soil surface state are depicted in Figure 5.

a. Site layout of high-speed photography b. Soil surface condition after subsoiling

Figure 5 High-speed photographic recording process

4 Results and discussion

4.1 High-speed photographic analysis of the influences of rake angle on the soil disturbance occurred

4.1.1 The influences of rake angle on the soil disturbance state

The soil disturbance states in the subsoiling strip were obviously different between the subsoiling treatments with different rake angles. High-speed photographic images of two rake angles were selected to show the differences in soil disturbance states at the different Moments (Figure 6). Moment 1 is the time when the subsoiler was preparing to enter the image collecting region, at Moment 2, the subsoiler completely entered the image collecting region, Moment 3 is the time at which the subsoiler reached the centre of the image collecting region, at Moment 4, the subsoiler was leaving the image collecting region, and the subsoiler completely exited the image collecting region at Moment 5.

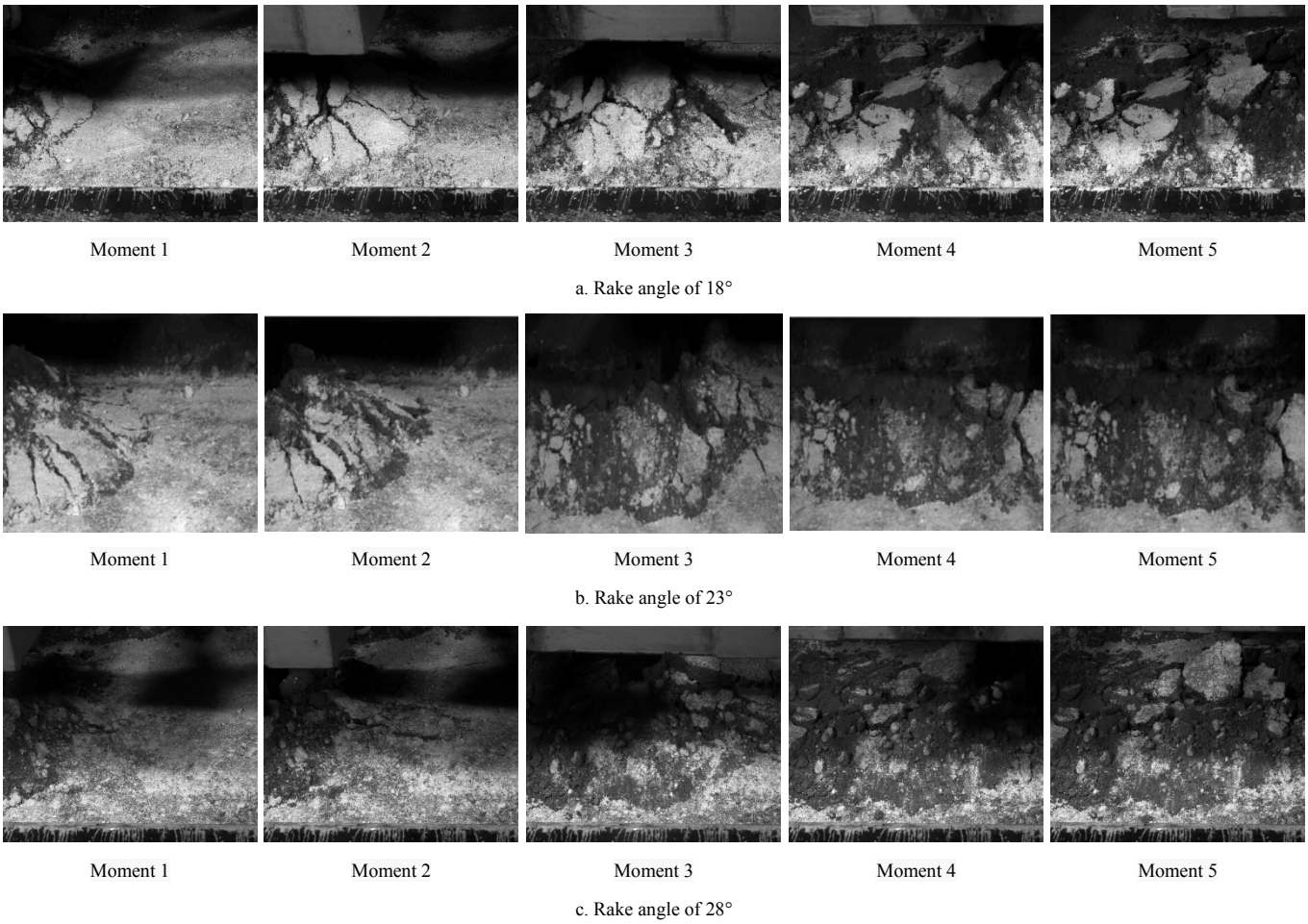

Figure 6 Images of soil disturbance state at different moments for two different rake angles

As shown in Figure 6, soil disturbance region on the surface had a fan shape. Differences existed in the sizes of the soil cracks and the post subsoiling ground surface soil disturbance states between the rake angles of 23°and 28°. Among these differences, the degree of soil disturbance after subsoiling with a rake angle of 28° was higher than the degree of soil disturbance with rake angle of 23°, and also 18° (images not shown for 18°). This occurred because the soil pushing effect increased and the soil uplift effect decreased as the rake angle increased. Under the test conditions, when the rake angle was smaller, the height of the soil raised by the subsoiler was higher. The soil disturbance range in the horizontal direction was larger when the rake angle was larger. Meanwhile, within a certain range, the soil failure surface increases as the rake angle increases. This increase changes the intra-soil interactions and the size of the disturbance range, which influences the soil disturbance range of the subsoiler.

Based on the high-speed recorded images, the following phenomena were observed: when the subsoiler operated with a rake angle of α, the subsoiler tine compressed the soil towards the front and upward along the direction opposite the positive force, F, of the subsoiler tine. The subsoiler edge cuts into the soil, and the soil body cracks when the shear force on a certain cross sectional surface reached the soil shear strength. At this point, the soil experienced shear damage that was apparent in the fan shaped disturbance region on the ground surface. The fan shape gradually expanded as the subsoiler advanced. As subsoiling continued, the soil was pushed forward and sideways by the surface of the subsoiler perpendicular to the subsoiler side wing surface. The soil structure fractured and formed soil blocks. The soil experienced the effects of the frictional force along the side wing of the subsoiler tine, due to the subsoiler tine moved backward. Due to the shearing effect of the cutting edge of the subsoiler shank, the compression effect of the straight shank segment, and the intra-soil interaction in the movement, the soil blocks were further

broken and crushed.

4.1.2 Influences of rake angle on the soil disturbance range

Figure 6 only qualitatively reflects the soil disturbance state influenced by the different rake angles at different Moments from a macroscopic viewpoint. To quantify the soil disturbance, images of the critical state in which the soil was being fractured but has not completely broken were selected for analysis. The *Calibrate* function of the *I-SPEED Suite* software was used to measure the horizontal distance of soil loosening by the subsoiler at different rake angles. This horizontal soil loosening distance was used to express the influences of the subsoiler on the soil disturbance range in the vertical surface. The measured results by *I-SPEED Suite Calibrate* and *Annotations* are shown in Figure 7. In Figure 7, the rectangle is the position of the subsoiler shank. The horizontal soil loosening distance was measured on the soil surface from the point 1 (the front edge of the disturbed soil) to the point 2 (on the vertical line of the subsoiler shank) (Figure 7a). The raised soil in the front of subsoiler was quantified by the soil raising angle (Figure 7b) that reflected the uplifting function of the subsoiler.

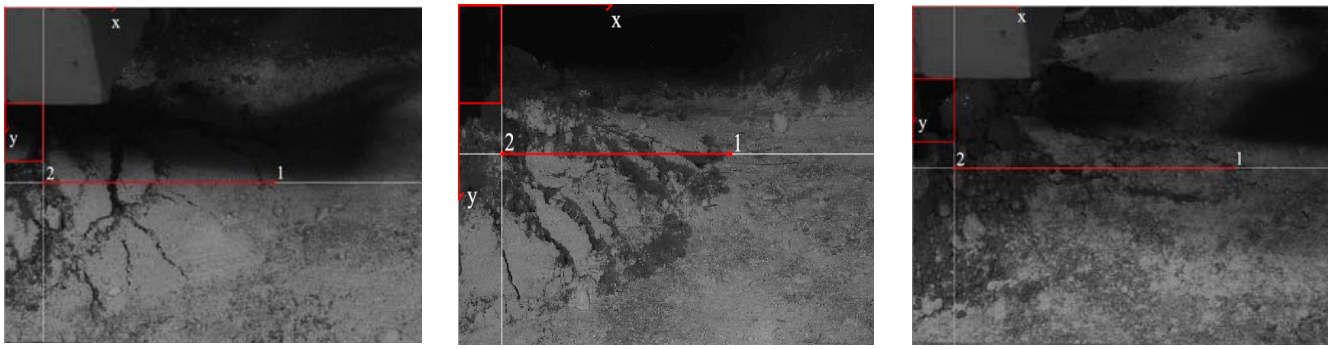

Rake angle of 18 ° Rake angle of 23° Rake angle of 28 °

a. The horizontal soil loosening distance

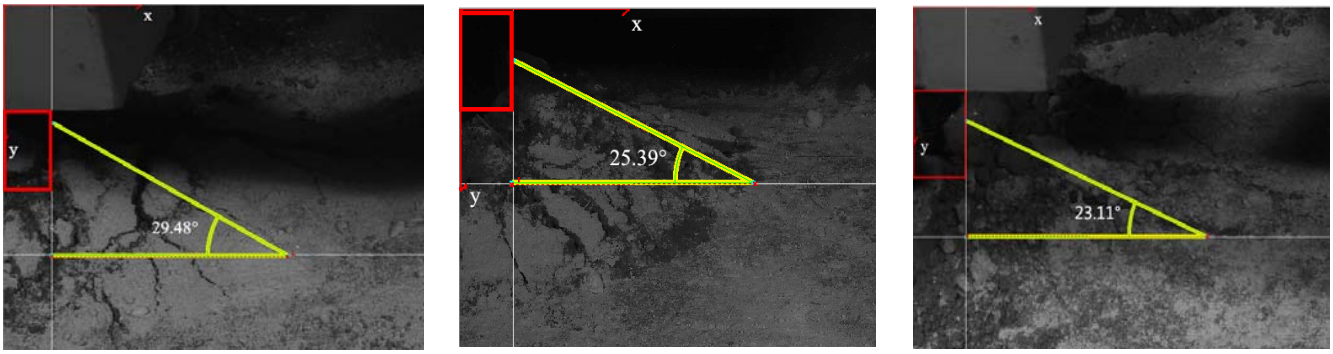

Rake angle of 18 ° Rake angle of 23° Rake angle of 28 °

b. The included angle between inclined plane of the ridge and horizontal plane

Figure 7 The measurement results of *I - SPEED Suite Calibrate* and *Annotations*

When the rake angles were 18º, 23º, and 28º, the horizontal soil loosening distance were 495 mm, 540 mm, and 632 mm (The distance of line segment 12 in Figure 7a is measured by the Calibrate function of the *I-SPEED Suite* software) respectively, meaning that the horizontal soil disturbance range increased as the rake angle was increased. The corresponding soil raising angles were 29.48º, 25.39º, and 23.11º. Thus, the height of the soil uplift resulting from the subsoiler decreased as the rake angle increased. These results are consistent with the mechanisms by which rake angle impacted soil disturbance discussed above. Therefore, the changes in the soil pushing force, soil uplift force, and soil movement speed with the rake angle are considered to be responsible for these phenomena. This is consistent with the results of McKyes (1985).

4.1.3 Influences of the subsoiler rake angle on the amount of soil disturbance

To further analyse the influence of the rake angle on soil disturbance in the subsoiling strip, the amounts of soil disturbance were calculated for the different rake angles based on the ground surface to subsoiling furrow

cross sectional contour before subsoiling.

According to test measurements, the cross-sectional area formed by the pre-subsoiling ground surface and subsoiling furrow for the rake angles of 18º, 23º, and 28º were calculated as 774.4 cm^2, 882.5 cm^2, and 854.1 cm^2, respectively. This indicated that when the subsoiling strip length was constant, the soil disturbance area when using the rake angle of 23º was 1.14 and 1.03 times the soil disturbance area when using the rake angles of 18º and 28º, respectively. This phenomenon occurred because the thickness of the disturbed soil increased as the rake angle α increased ($18º<\alpha<28º$) when the intra-soil disturbance was not considered; thus, a certain change in the soil disturbance area was induced. In practical operation processes, soil cones and soil heels form where the subsoiler tine and shank are connected when the rake angle is too large or too small, which reduces the cross sectional area of the soil disturbance.

4.2 Influences of subsoiler rake angle on soil disturbance rate

In the above discussion, high-speed photograph recordings showed that subsoiling operations with different rake angles produced obviously different soil disturbance characteristics, such as horizontal soil loosening distance and soil disturbance area. In this section, soil-disturbance rate was discussed to further assess effects of rake angle. The soil-disturbance rates for 10 cm and the full tillage layer (30 cm) were obtained from Equations (5) and (6) for different rake angles, and they are listed in Table 1.

Table 1 Soil-disturbance rate of subsoiler with different rake angles

Topsoil range	Rake angle, °	Soil-disturbance rate, %
10 cm topsoil	18	85.35
	23	88.14
	28	92.89
30 cm topsoil	18	95.86
	23	97.13
	28	99.13

A higher disturbance rate indicates a better performance of the subsoiler. As shown in Table 1, the subsoiler performance improved as the rake angle increased. The rake angle of 28º was the best, as it resulted in the highest disturbance rate in both the 10 cm and full tillage layers. Because the soil disturbance effect is the result of the combined effect of soil uplift and pushing by the subsoiler, and the rake angle affects the pushing and uplifting forces, the subsoiler with a larger rake angle would be more aggressive, in terms of soil disturbance. As the result, it increased the degree of soil disturbance. Meanwhile, the research of Xue et al. (1987) showed that a smaller rake angle negatively affected the subsoiler soil disturbance performance. Thus, a reasonably large rake angle can improve the subsoiler soil disturbance performance.

5 Conclusions

In this study, the high-speed photography technology was used to understand the mechanisms by which the rake angle of an arrow subsoiler affected the soil disturbance process. Conclusions were drawn as the following:

(1) Rake angle was the main factor influencing the soil disturbance process. Changing rake angle could induce changes in the interactions between subsoiler and soil, thereby impacts soil disturbance process. The soil pushing force increases and the soil uplift force decreased as the rake angle increased.

(2) When the rake angle was increased, the horizontal soil loosening distance increased while the soil raising angle shows a decreasing trend.

(3) For a fixed soil loosening strip length, the soil disturbance area resulting from a subsoiler rake angle of 23° was 1.14 and 1.03 times greater than those resulted from the rake angles of 18° and 28°, respectively.

(4) When the rake angle of subsoiler was 18°, 23° and 28°, the soil-disturbance rate in the top 10 cm soil layer was 85.35%, 88.14%, and 92.89% respectively, and that in the entire topsoil layer was 95.86%, 97.13% and 99.13% respectively.

In general, increasing rake angle in a practical range can improve soil disturbance effectiveness and tillage quality of subsoiler.

Acknowledgements

This work was supported by Scientific and technological project in Shaanxi Province (no. 2013K02-11), Science and technology planning project of Yangling demonstration area (no. 2014NY-29) and Key

project of Northwest Agriculture and Forestry University (no. 00900-Z101021501).

References

Badegaonkar, U. R., G. Dixit, and K. K. Pathak, 2010. An experimental investigation of cultivator shank shape on draft requirement. *Archives of Applied Science Research*, 2(6): 246–255.

Gill, W. R., and G. E. Vanden Berg. 1967. *Tillage and Soil Dynamics*. Washington, D.C.: Agricultural Research Service, U.S. Dept. of Agriculture.

Godwin, R. J., 2007. A review of the effect of implement geometry on soil failure and implement forces. *Soil and Tillage Research*, 97(2): 331–334.

Godwin, R. J., and M. J. O'Dogherty. 2007. Integrated soil tillage force prediction models. *Journal of Terramechanics*, 44(1): 3–14.

Hamza, M. A., and W. K. Anderson. 2005. Soil compaction in cropping systems: A review of the nature, causes and possible solutions. *Soil and Tillage Research*, 82(2): 121–145.

He, J., Q. J. Wang, H. W. Li, L. J. Liu, H. W. Gao, 2009. Effect of alternative tillage and residue cover on yield and water use efficiency in annual double cropping system in North China Plain. *Soil and Tillage Research*, 104(1): 198–205.

Huang, Y., C. Hang, W. Li, P. Zhang, and R. Zhu. 2015. Subsoiling test and evaluation methodology study of tillage quality. *Journal of Northwest Sci-tech University of Agriculture and Forestry*, 43(11): 228–234.

Ibarra, S. Y., E. McKyes, and R. S. Broughton. 2005. A model of stress distribution and cracking in cohesive soils produced by simple tillage implements. *Journal of Terramechanics*, 42(2): 115–139.

JB/T 10295-2014. *Combined Implement for Subsoiler and Cultivating*. Ministry of Industry and Information Technology of the People's Republic of China, Chin.

JB/T 9788-1999. *Chiselling Subsoiler and Handle of Chiselling Subsoiler*. State Bureau of Machine-Building Industry, Chin.

Li, X., D. Zhang, W. Wang, T. Cui, and M. Tang. 2015. Optimization and experiment on performance parameters of forced-vibration subsoiler. *Transactions of the Chinese Society of Agricultural Engineering*, 31(21): 17–24.

Li, X., M. Tang, D. Zhang, W. Wang, and T. Cu. 2014. Effects of sub-soiling on soil physical quality and corn yield. *Transactions of the Chinese Society of Agricultural Engineering*, 30(23): 65–69.

McKyes, E. 1985. *Soil Cutting and Tillage*. Amsterdam: Elsevier Science Ltd.

Mouazen, A. M., and M. Nemenyi. 1999. Finite element analysis of subsoiler cutting in non-homogeneous sandy loam soil. *Soil and Tillage Research*, 51(1): 1–15.

Naeem, A., and G. Q. Fayyaz-ul-hassan. 2007. Effect of subsurface soil compaction and improvement measures on soil properties. *International Journal of Agriculture and Biology*, 9(3): 509–513.

Ouyang, Y., T. Hong, J. Su, N. Xu, X. Ni, and C. Yang. 2014. Design and experiment for rope brake device of mountain orchard traction double-track transporter. *Transactions of the Chinese Society of Agricultural Engineering*, 30(18): 22–29.

Perfect, E., M. Diaz-Zorita, and J. H. Grove. 2002. A prefractal model for predicting soil fragment mass-size distributions. *Soil and Tillage Research*, 64(1): 79–90.

Qi, G., L. Liu, Y. Zhao, Z. Gong, Y. Q. Yang, and Y. Yang. 2015. Effects of subsoiler's rake depth and spade shape on traction resistance. *Journal of Agricultural Mechanization Research*, 37(11): 161–165.

Quan, L., D. Zhang, B. Zeng, J. Tong, and D. Chen. 2013. Modeling and optimizing dither mechanism for conveying corn stubble. *Transactions of the Chinese Society of Agricultural Engineering*, 29(3): 23–29.

Shahgoli, G., C. Saunders, J. Desbiolles, and J. Fielke. 2009. The effect of rake angle on the performance of oscillatory tillage. *Soil and Tillage Research*, 104(1): 97–105.

Shahgoli, G., J. Fielke, J. Desbiolles, and C. Saunders. 2010. Optimising oscillation frequency in oscillatory tillage. *Soil and Tillage Research*, 106(2): 202–210.

Wang, H. J., J. P. Hao, R. Y. Feng, Y. Nan, S. Q. Yang, and J. F. Nan. 2015. Micro-hole subsoiling decreasing soil compaction, and improving yield and seed quality of cotton. *Transactions of the Chinese Society of Agricultural Engineering*, 31(8): 7–14.

Wang, W. 2011. Cultivator layered subsoiling technology research and finite element analysis of subsoiling components. Ph.D. diss. China, Shenyang: Shenyang Agricultural University.

Xin, L., C. Li, J. Liang, and Z. Xing. 2014. Vibrating drag reduction considering acting force of piecewise soil. *Transactions of the Chinese Society for Agricultural Machinery*, 45(2): 136–140.

Xue, H., L. Yang, D. Lian, and B. Lu, 1987. Tests of designing parameters of double-wing subsoiler. *Journal of Northwest Sci-tech University of Agriculture and Forestry*, 15(1): 24–29.

Yang, Y., H. Zhang, T. Feng, Q. Lin, M. Xue, Z. Li, W. He, and X. Mi. 2012. Topsoil and subsoil combined cultivator and top-soiling experiment. *Journal of Mechanical Engineering*, 48(19): 163–168.

Zhang, J., J. Tong, and Y. Ma. 2014. Design and experiment of bionic anti-drag subsoiler. *Transactions of the Chinese Society of Agricultural Machinery*, 45(4): 141–145.

Zheng, H., J. Zheng, L. Yang, R. Li, W. Li, H. Wang, H. Ren, H. Qi, and W. Liu. 2015. Change characteristic of soil compaction of long-term different tillage methods in cropland. *Transactions of the Chinese Society of Agricultural Engineering*, 31(9): 63–70.